Inhibition of monocarboxyate transporter 1 by AZD3965 as a novel therapeutic approach for diffuse large B-cell lymphoma and Burkitt lymphoma

Richard A. Noble,[1] Natalie Bell,[1] Helen Blair,[1] Arti Sikka,[2] Huw Thomas,[1] Nicole Phillips,[1] Sirintra Nakjang,[1] Satomi Miwa,[3] Rachel Crossland,[1] Vikki Rand,[1] Despina Televantou,[4] Anna Long,[4,5] Hector C. Keun,[2] Chris M. Bacon,[1,4,5] Simon Bomken,[1,6] Susan E. Critchlow[7] and Stephen R. Wedge[1]

[1]Northern Institute for Cancer Research, Newcastle University, Newcastle upon Tyne; [2]Division of Cancer, Imperial College London; [3]Institute for Cell and Molecular Biosciences, Newcastle University, Newcastle upon Tyne; [4]Cellular Pathology, Newcastle upon Tyne Hospitals NHS Foundation Trust; [5]MRC/EPSRC Newcastle Molecular Pathology Node, Newcastle upon Tyne; [6]Department of Pediatric and Adolescent Hematology and Oncology, Newcastle upon Tyne Hospitals NHS Foundation Trust and [7]AstraZeneca, Cambridge, UK

 doi:10.3324/haematol.2016.163030

Received: December 22, 2016.

Accepted: March 31, 2017.

Pre-published: April 6, 2017.

Correspondence: steve.wedge@ncl.ac.uk

Supplementary Information

Inhibition of monocarboxyate transporter 1 by AZD3965 as a novel therapeutic approach for the treatment of diffuse large B-cell lymphoma and Burkitt lymphoma

Authors

Richard A. Noble[1], Natalie Bell[1], Helen Blair[1], Arti Sikka[2], Huw Thomas[1], Nicole Phillips[1], Sirintra Nakjang[1], Satomi Miwa[3], Rachel Crossland[1], Vikki Rand[1], Despina Televantou[4], Anna Long[4,5], Hector C. Keun[2], Chris M. Bacon[1,4], Simon Bomken[1,6], Susan E. Critchlow[7] and Stephen R. Wedge[1].

Authors' Affiliations

[1]Northern Institute for Cancer Research, Newcastle University, Newcastle upon Tyne, UK

[2]Division of Cancer, Imperial College London, London, UK

[3]Institute for Cell and Molecular Biosciences, Newcastle University, Newcastle upon Tyne, UK

[4]Cellular Pathology, Newcastle upon Tyne Hospitals NHS Foundation Trust, UK

[5]MRC/EPSRC Newcastle Molecular Pathology Node, Newcastle upon Tyne, UK

[6]Department of Pediatric and Adolescent Hematology and Oncology, Newcastle upon Tyne Hospitals NHS Foundation Trust

[7]AstraZeneca, Cambridge, UK.

Corresponding author: Steve Wedge, Northern Institute for Cancer Research, Newcastle University, Paul O'Gorman Building, Medical School, Framlington Place, Newcastle upon Tyne, NE2 4HH, UK. Phone: 440-1912084418; E-mail: steve.wedge@ncl.ac.uk

Supplemental Methods

Cell culture, drug and antibody preparation

Farage, Pfeiffer and Toledo were obtained from ATCC (Manassas, VA, USA) and BL-41, BJAB, CA46, Daudi, OCILY18, Raji and Ramos from DSMZ (Braunschweig, Germany). RIVA were obtained from Prof Alison Banham, (University of Oxford). All cell lines were re-authenticated at the end of the study by short tandem repeat (STR) analysis (New Gene, Newcastle upon Tyne). All cell lines were cultured in RPMI-1640 media (Sigma, St Louis, MO, USA) supplemented with 10% fetal calf serum (Gibco).

For *in vitro* experiments, AZD3965 (AstraZeneca, Cambridge, UK) was prepared as a 10mM stock solution in dimethyl sulfoxide (DMSO) and BAY 87-2243 (SelleckChem, Houston, TX, USA) was prepared at 1 mM in ethanol. All *in vitro* experiments were vehicle-controlled with a final concentration of 0.01% DMSO or 0.01% ethanol. For *in vivo* studies, AZD3965 and BAY 87-2243 were formulated as previously described.[1, 2]

Antibodies used for Western blotting were GAPDH (FL-335), MCT4 (H-90) and PARP (H-250) (Santa Cruz, Dallas, TX, USA) and CD147 (UM-8D6) (Ancell, Bayport, MN, USA). MCT1 antibodies used were (C-20) Santa Cruz) and (20139-1-AP) (Proteintech, Manchester, UK). For immunohistochemical analysis, monoclonal MCT1 and MCT4 antibodies were used (AstraZeneca, Cambridge, UK).

Determination of oxygen consumption rate (OCR) and extracellular acidification rate (ECAR)

Cells were maintained in cell Seahorse Base Media without FCS, or bicarbonate, and incubated for 45min in a non-CO_2 incubator at 37°C. The wells were mixed for 2min and the pH and oxygen concentration measured every 22 seconds for 3min. Compounds were injected into the wells via reagent delivery ports to give predetermined final concentrations; AZD3965 (100 nM), BAY 87-2243 (100 nM), oligomycin (Sigma, 1 µg/mL), carbonyl cyanide 4(trifluoromethoxy)phenylhyrazone (FCCP) (Sigma, 300 nM) and antimycin A (Sigma, 2.5 µM). After each addition, two data points of 3min were taken to determine the OCR (pM O_2/min) and ECAR (mpH/ min), with data being normalised to protein concentration.

Oligomycin treatment, which inhibits ATP generation, revealed that this increased OCR reflects increased oxygen consumption coupled to ATP generation in CA46-R. In addition to an increase in basal OCR, the reserve oxidative capacity of CA46-R greatly exceeded that of parental CA46 cells, as indicated by their response to the protonophore FCCP (Figure 4C). Since the basal respiratory production of CO_2 from OCR can also contribute to ECAR, the glycolytic rate of CA46-R cells may be even less than inferred from our measurement of ECAR.[3]

Metabolite determination using nuclear Magnetic Resonance (NMR)

High Resolution One dimensional (1D) ^{1}H NMR spectra were acquired using a Bruker AVANCE spectrometer (Bruker Bio Spin) at 298K, 14.1 T and 400 MHz ^{1}H frequency using a 4,4-dimethyl-4-silapentane-1-sulfonic acid (DSS) internal standard prepared in deuterated water. All spectra were acquired using a single pulse experiment with solvent presaturation, 32 free induction decays (FIDs), a spectral width of 6402.049 Hz, 64K complex data points and a recycle delay of 4 seconds. Spectra were

processed with 0.3 Hz line broadening. Peaks were integrated and resonances assigned to metabolites using spectral comparison with the Human Metabolome Database (HMDB). The metabolite composition of spent and fresh media were compared using CORE profiling with normalisation to cell number as previously described.[4]

Metabolite determination using gas chromatography mass spectrometry (GCMS)

For metabolite extraction samples were kept on dry ice throughout. Tumor samples were weighed and added to screw-cap tubes containing 0.1 mm glass beads. Pre-chilled 80% methanol (800 µL) was added and samples homogenised using a Precellys 24 bead beater (Bertin Technologies). Supernatants were collected after centrifugation (12 000 x g, 5min, at 4°C). The extraction was repeated and the fractions for each sample were pooled. Supernatants were then dried in a vacuum concentrator and subjected to dual-phase extraction. 300 µL of chloroform/methanol (2:1) was added to each sample followed by vortexing. 300 µL of water was then added to each sample followed by vortexing and centrifugation (21 000 x g, 10min at 4°C). The aqueous (upper) layer from each sample was transferred to silanized GC-MS vials. The dual-phase extraction was repeated and fractions were pooled for each sample. Tumor sample extract (20 mg) was dried in a vacuum concentrator and analysed by GC-MS.

GC-MS analysis was performed using in-house protocols (Imperial College London).[5] Metabolites intensities were normalised to a myristic acid-d27 internal standard. Metabolite extracts were derivatized using the two-step method of derivatisation: methoxymation and silylation.[6] When required, samples were diluted with anhydrous pyridine. Samples were analysed in a splitless mode on an Agilent

7890 GC with a 30m DB-5MS capillary column and a 10m Duraguard column, coupled to an Agilent 5975 MSD. Metabolites were assigned using FiehnLib assisted processing in AMDIS[6, 7] and manually assessed using the Gavin package.[5]

Supplemental References

1. Polanski R, Hodgkinson CL, Fusi A, et al. Activity of the Monocarboxylate Transporter 1 Inhibitor AZD3965 in Small Cell Lung Cancer. Clin Cancer Res. 2014;**20**(4):926-937.

2. Schockel L, Glasauer A, Basit F, et al. Targeting mitochondrial complex I using BAY 87-2243 reduces melanoma tumor growth. Cancer Metab. 2015;**3**:11.

3. Mookerjee SA, Goncalves RLS, Gerencser AA, Nicholls DG, Brand MD. The contributions of respiration and glycolysis to extracellular acid production. Biochimica et Biophysica Acta (BBA) - Bioenergetics. 2015;**1847**(2):171-181.

4. Jain M, Nilsson R, Sharma S, et al. Metabolite profiling identifies a key role for glycine in rapid cancer cell proliferation. Science. 2012;**336**(6084):1040-1044.

5. Behrends V, Tredwell GD, Bundy JG. A software complement to AMDIS for processing GC-MS metabolomic data. Anal Biochem. 2011;**415**(2):206-208.

6. Kind T, Wohlgemuth G, Lee DY, et al. FiehnLib: mass spectral and retention index libraries for metabolomics based on quadrupole and time-of-flight gas chromatography/mass spectrometry. Anal Chem. 2009;**81**(24):10038-10048.

7. Stein SE. An integrated method for spectrum extraction and compound identification from gas chromatography/mass spectrometry data. Journal of the American Society for Mass Spectrometry. 1999;**10**(8):770-781.

8. Barretina J, Caponigro G, Stransky N, et al. The Cancer Cell Line Encyclopedia enables predictive modelling of anticancer drug sensitivity. Nature. 2012;**483**(7391):603-607.

9. Luo W, Brouwer C. Pathview: an R/Bioconductor package for pathway-based data integration and visualization. Bioinformatics. 2013;**29**(14):1830-1831.

Supplemental Figures

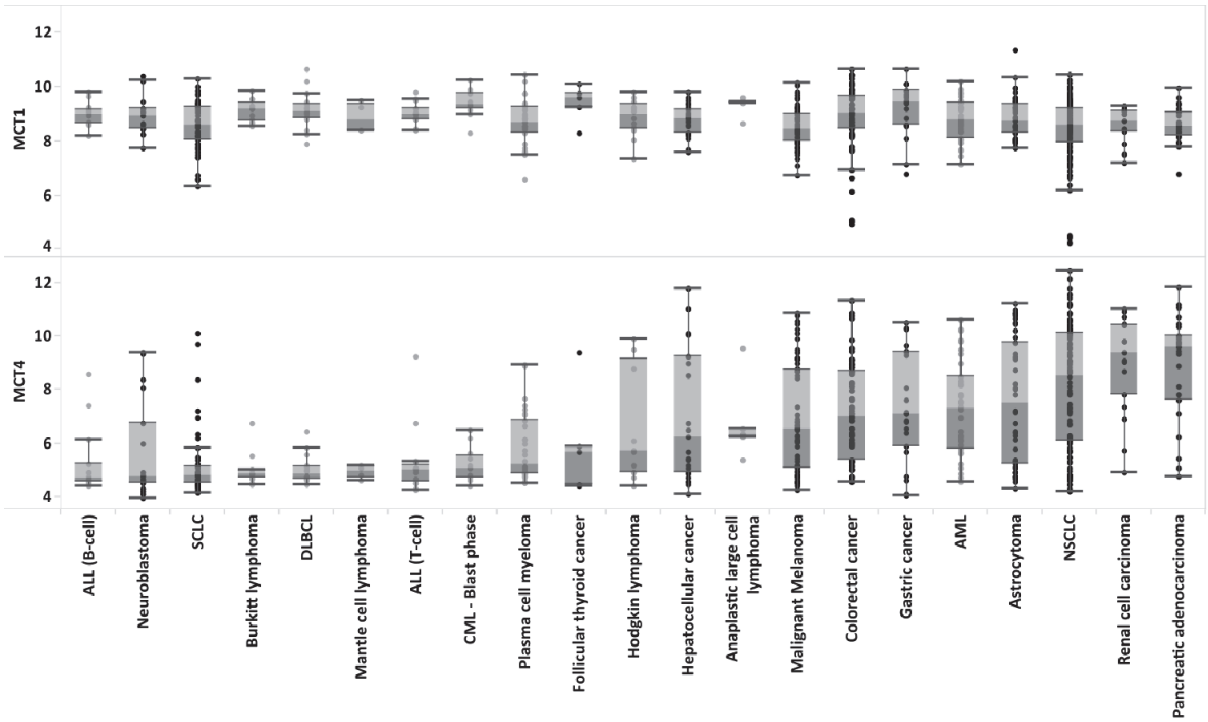

Figure S1: Cancer cell line expression of MCT1 and MCT4

RMA-normalised mRNA expression of MCT1 and MCT4 in hematological ■ and solid tumor ■ cell lines. Data from the Cancer Cell Line Encyclopaedia.[8]

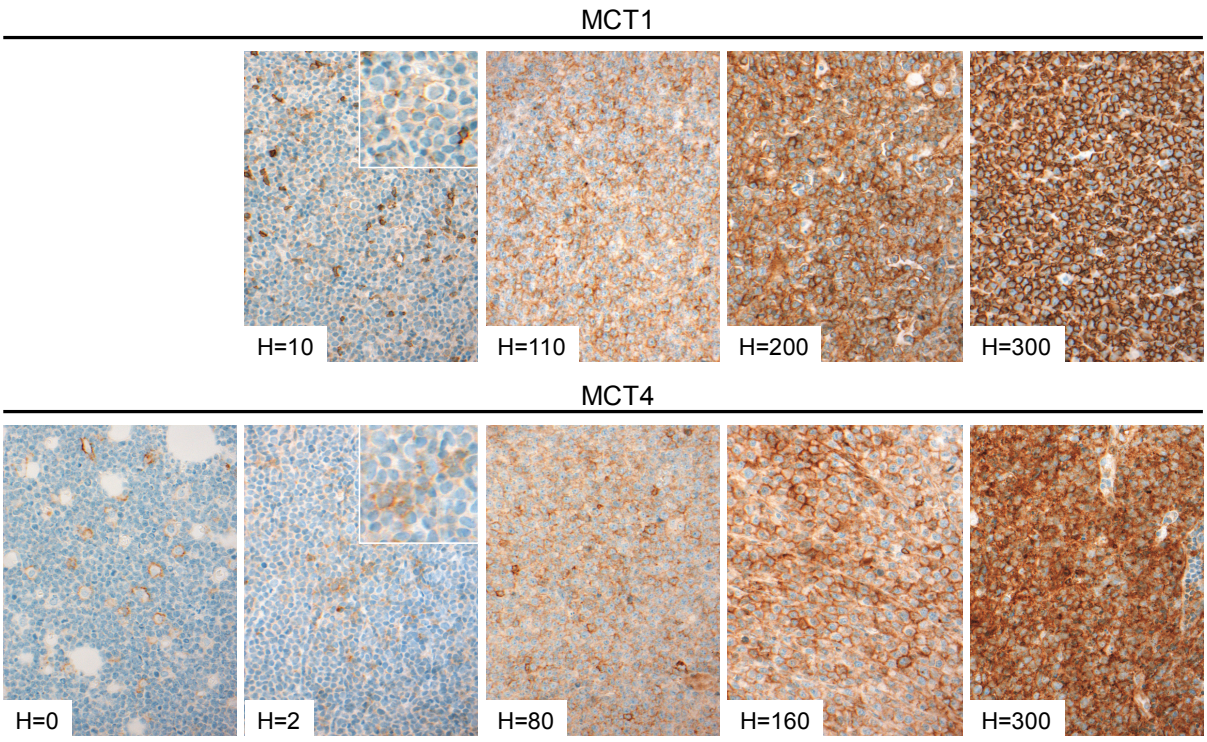

Figure S2: MCT1 and MCT4 staining of DLBCL patient samples

Immunohistochemical staining of MCT1 and MCT4 was performed and H-scores determined as detailed in the Methods section of the main manuscript. Panels show representative images from lymphomas with H-scores within each category (0, 1-10, 11-100, 101-200, 201-300). H-scoring considered only scoring on tumor cells. An MCT1 H-score of 0 was not recorded for any of the 120 samples examined. The lymphoma with an MCT1 H-score of 10 shown, comprised small strongly positive lymphocytes and macrophages with only a few weakly positive tumour cells (inset). The representative MCT4 H-score of 0 shows staining on positive macrophages only and the MCT4 H-score of 2 shown is indicative of weak sporadic tumour cell staining (inset).

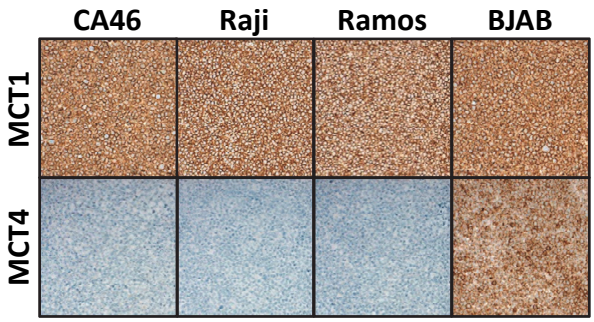

Figure S3: Cancer cell line expression of MCT1 and MCT4

Immunohistochemical staining of MCT1 and MCT4 in a sub-set of B-NHL cell lines

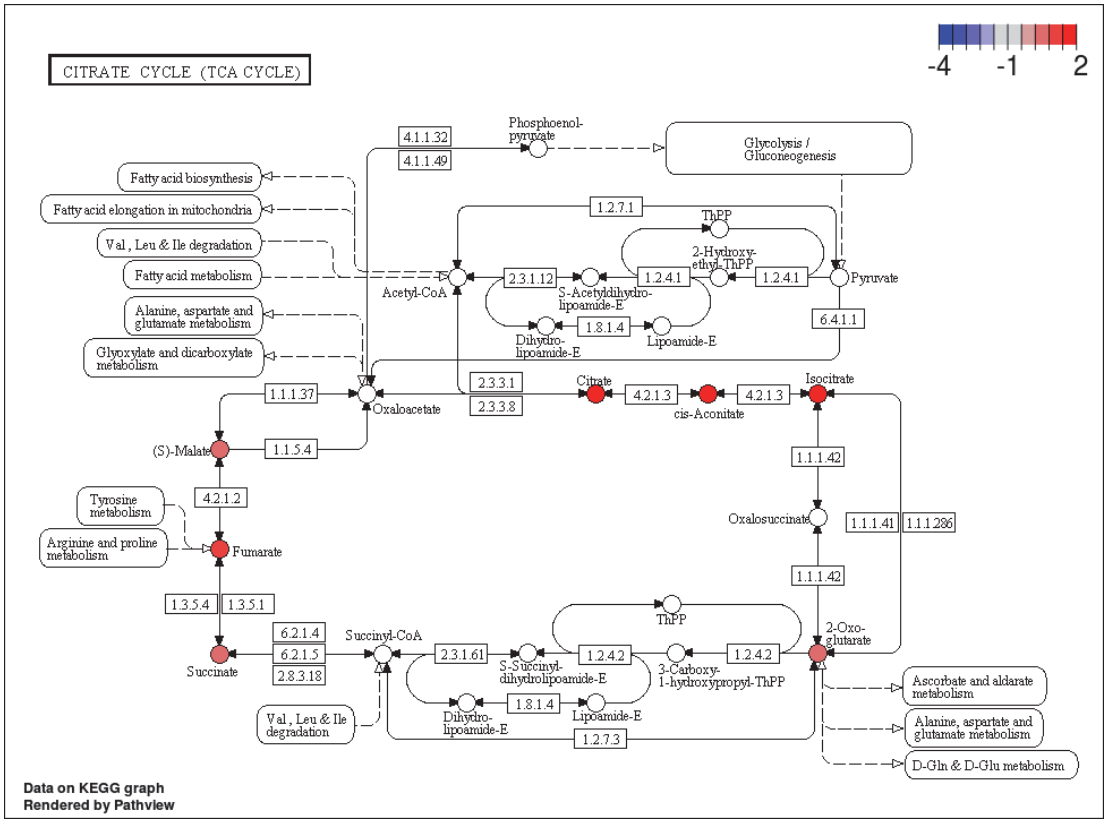

Figure S4: AZD3965 increases levels of TCA cycle intermediates

Enrichment in TCA cycle intermediates in CA46 cells following 2h exposure to AZD3965 (100 nM), significant alterations relative to vehicle treated control (Log_2FC) mapped to KEGG pathways using Pathview.[9]

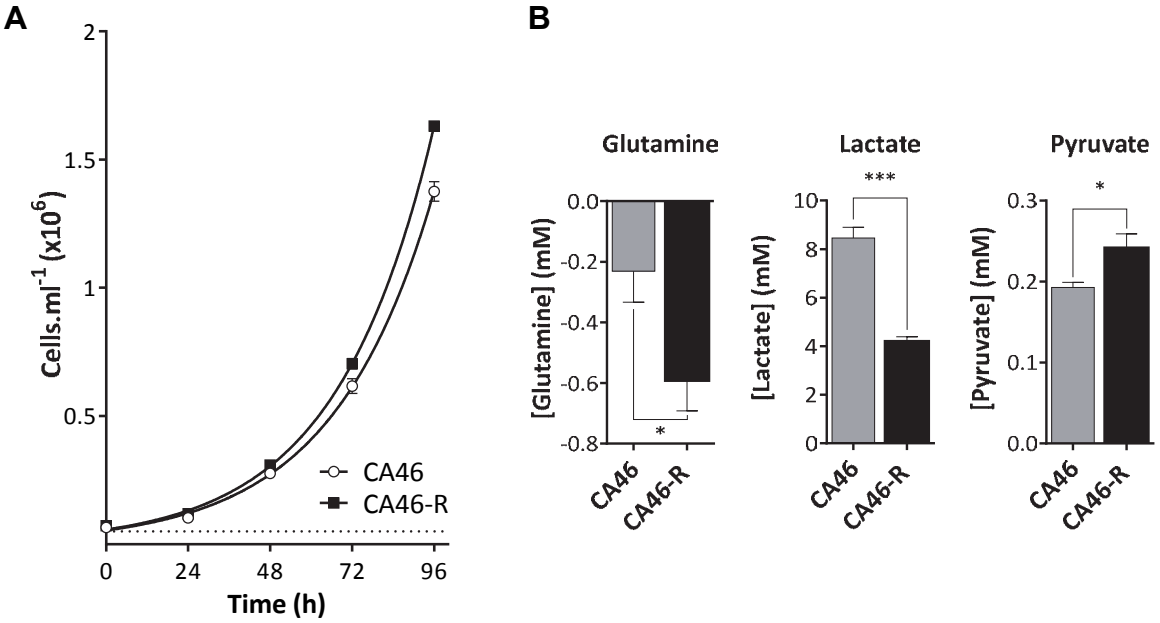

Figure S5: AZD3965 resistant CA46-R do not exhibit an altered proliferative rate.

CA46 and CA46-R proliferation rates were assessed by daily cell counts (0-96h). Mean of three independent experiments ± SEM. Analysis of culture media (24h incubation) from untreated CA46 and CA46-R cells. Metabolite concentrations (mM) are shown per $1x10^6$ cells.

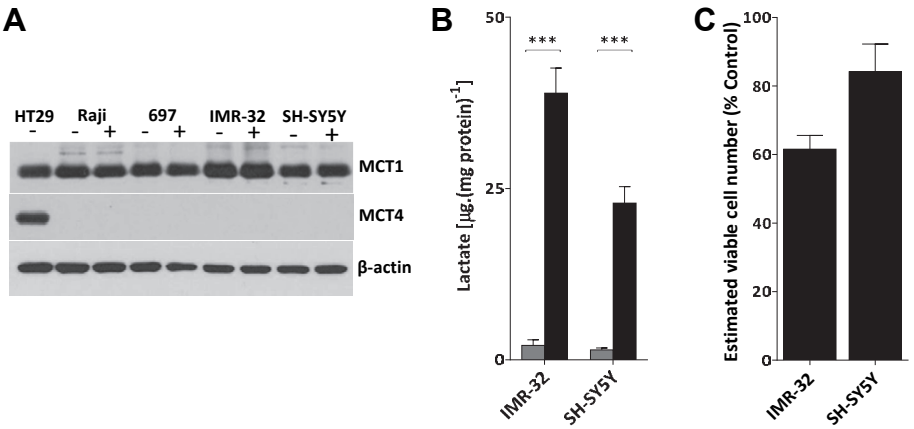

Figure S6: Low MCT4 expression is not sufficient for MCT1 inhibition to be efficacious.

(**A**) Expression of MCT1 and MCT4 protein following treatment with AZD3965 (1 µM for 72h) in neuroblastoma (IMR-32 and SH-SY5Y), BL (Raji) and B-ALL (697). HT-29 was used as an MCT4 positive control. β-actin was used as a loading control. (**B**) Intracellular lactate was measured in cells following exposure to AZD3965 (1 µM) or DMSO vehicle for 72h. (**C**) Cells were treated with AZD3965 (1 µM) for 72h and sensitivity assessed by XTT assay. Data are expressed relative to vehicle treated control. All data represent mean ± SEM of 3 independent experiments.